

# Role of $\gamma$ -Kafirin in the Formation and Organization of Kafirin Microstructures

Joseph O. Anyango, John R. N. Taylor, and Janet Taylor\*

Institute for Food, Nutrition and Well-being and Department of Food Science, University of Pretoria, Private Bag X20, Hatfield 0028, South Africa

**ABSTRACT:** The possible importance of the cysteine-rich  $\gamma$ -prolamin in kafirin and zein functionality has been neglected. The role of  $\gamma$ -kafirin in organized microstructures was investigated in microparticles. Residual kafirin (total kafirin minus  $\gamma$ -kafirin) “microparticles” were non-discrete (amorphous mass of material), as viewed by electron microscopy and atomic force microscopy. Adding 15%  $\gamma$ -kafirin to residual kafirin resulted in the formation of a mixture of non-discrete material and nanosize discrete spherical structures. Adding 30%  $\gamma$ -kafirin to the residual kafirin resulted in discrete spherical nanosize particles. Fourier transform infrared spectroscopy indicated that  $\gamma$ -kafirin had a mixture of random-coil and  $\beta$ -sheet conformations, in contrast to total kafirin, which is mainly  $\alpha$ -helical conformation.  $\gamma$ -Kafirin also had a very high glass transition temperature ( $T_g$ ) ( $\approx 270$  °C). The conformation and high  $T_g$  of  $\gamma$ -kafirin probably confer structural stability to kafirin microstructures. Because of its ability to form disulfide cross-links,  $\gamma$ -kafirin appears to be essential to form and stabilize organized microstructures.

**KEYWORDS:** *Kafirin microparticles,  $\gamma$ -kafirin, disulfide cross-linking, glass transition temperature, secondary structure*

## INTRODUCTION

There is great interest in the use of kafirin and zein, the prolamin proteins of sorghum and maize, respectively, as functional proteins to make organized bioplastic structures, such as microparticles,<sup>1–3</sup> bioplastic films,<sup>2,4</sup> fibers,<sup>5,6</sup> sponges,<sup>7</sup> scaffolds,<sup>8</sup> and viscoelastic wheat-like doughs.<sup>9</sup> These structures have potential in biomedical applications for use as scaffolds for tissue repair<sup>8,10</sup> and for encapsulation of bioactives for controlled or delayed release of drugs<sup>11</sup> and nutraceuticals.<sup>12</sup> Potential food applications may include encapsulation of, for example, essential oils<sup>1</sup> or vitamins<sup>13</sup> and replacement of gluten in gluten-free formulations for celiac sufferers.<sup>9,14,15</sup> Bioplastic films may be used as semi-permeable membranes for food coating to extend perishable food shelf life.<sup>16</sup>

However, currently, there are few commercial products. Reasons for this include high cost and inferior and inconsistent functional properties compared to synthetic polymer plastics<sup>17</sup> and gluten in the case of baked goods.<sup>9</sup> Improvement of kafirin and zein functionality is challenging because of their complexity and lack of uniformity. A number of reviews have been published on kafirin and zein composition, structure, and functionality.<sup>17–19</sup> Briefly, they are small, highly folded proteins, which consist of four classes ( $\alpha$ -,  $\beta$ -,  $\gamma$ -, and  $\delta$ -), within which are several subclasses. They are usually considered hydrophobic proteins but have hydrophilic characteristics and are amphiphilic. Functional properties of their biopolymers are strongly affected by water and temperature.

Recent research indicates that protein aggregation plays a major role in the formation of zein and kafirin micro- or nanostructures<sup>17,20,21</sup> and that these nanostructures form the basis of the various bioplastic materials mentioned above.<sup>20</sup> Wang and Padua<sup>21</sup> suggested that assembly of  $\alpha$ -zein nanostructures is driven by the amphiphilic properties of zein and begins by the protein structure unfolding. The  $\alpha$ -helical structure of zein ( $\alpha$ -zein) unfolds into  $\beta$ -sheets, followed by

side-by-side placement of antiparallel  $\beta$ -sheets. These ribbon-like structures then curl into a ring stabilized by hydrophobic interactions, and the rings “grow” into nanospheres. However, there is inadequate knowledge as to how this happens. The protein secondary structure in terms of  $\alpha$ -helical and  $\beta$ -sheet structures seems to play a key but incompletely understood role. The  $\beta$ -sheet structures have been shown to be important in the stabilization of zein-based dough systems.<sup>14,15</sup> Zein contains a similar amount of  $\beta$ -sheet structure to gluten if mixed at 35 °C (above its glass transition temperature) and forms a viscoelastic polymer. However, unlike gluten, heat and shear are necessary to maintain this structure.<sup>14</sup> Stability of the zein dough could be retained with the addition of a small amount of  $\beta$ -sheet-rich co-protein.<sup>15</sup> Thus, the viscoelastic properties and relaxation rate of the zein polymers appear to be related to stable  $\beta$ -sheet structures.

The effects of the presence of the other prolamin classes, in particular  $\gamma$ -zein or  $\gamma$ -kafirin, with their high cysteine contents and subsequent ability to form intermolecular disulfide bonds during microstructure formation are of importance. It has been suggested that disulfide bonding through cysteine residues could stabilize kafirin microstructures,<sup>22,23</sup> in a similar order to that proposed for the stabilization of kafirin and zein protein bodies<sup>24,25</sup> but in a non-cellular system. For zein, the specific zein classes and order in which they are assembled is vital for normal spherical protein bodies to form.<sup>25</sup>  $\gamma$ -Zein synthesis is important for initiating protein body formation, retention of  $\alpha$ -zein within the protein body, and maintenance of the spherical orientation of the protein bodies.<sup>25</sup> Transgenic sorghum lines with downregulation of the synthesis of various combinations

**Received:** August 12, 2013

**Revised:** October 17, 2013

**Accepted:** October 22, 2013

**Published:** October 22, 2013



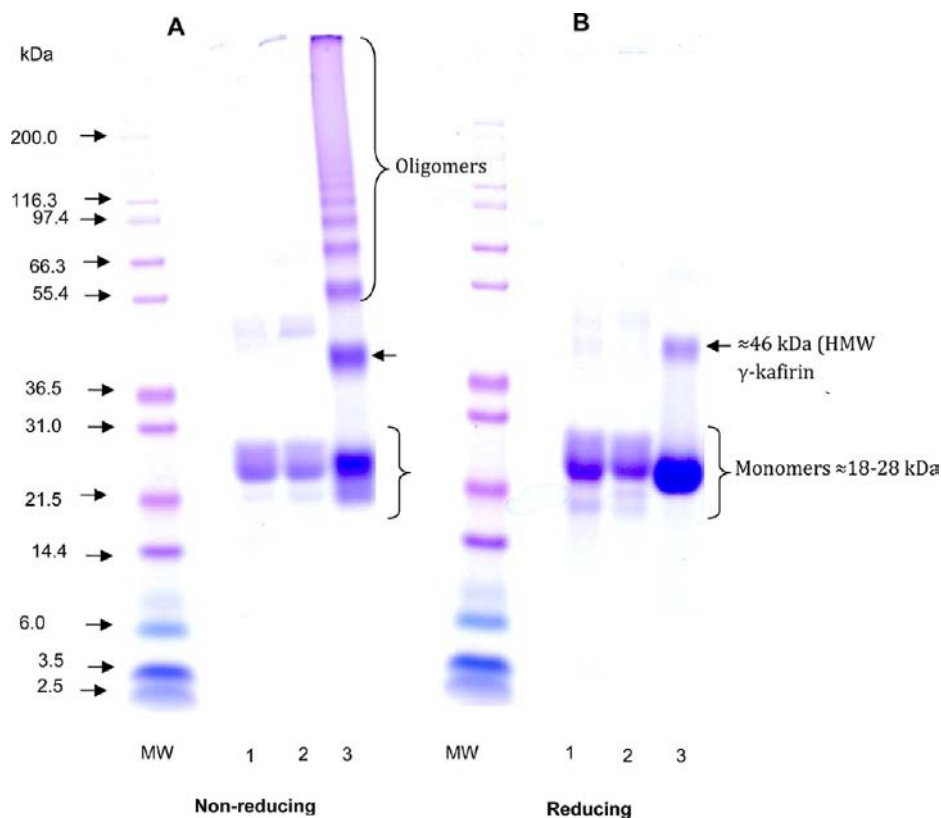


**Figure 1.** SDS-PAGE under (A) non-reducing and (B) reducing conditions of kafirin. Protein loading  $\approx 10 \mu\text{g}$ . Lanes MW, molecular markers; 1, total kafirin; 2, residual kafirin; and 3,  $\gamma$ -kafirin.

of kafirin classes have resulted in protein bodies with varying degrees of deformity.<sup>26–29</sup>

It also appears likely that the different prolamins may play specific roles in the formation and functionality of kafirin and zein structures. Schober et al.<sup>30</sup> found that zein, which was predominantly  $\alpha$ -zein, with approximately 10% co-extracted  $\beta$ - and  $\gamma$ -zein was the best for aggregation in warm water to produce a gluten-like material, whereas film formation was less sensitive to the presence of  $\beta$ - and  $\gamma$ -zein.

Using kafirin microparticles as an example of a prolamins bioplastic structure, this study describes the role of the  $\gamma$ -kafirin class in their formation and organization. Microparticles is a term used to collectively refer to microcapsules (single core surrounded by a layer of wall material) or microspheres (core dispersed in a continuous matrix network) with a size range of 1–250  $\mu\text{m}$ .<sup>31</sup> The information will be useful in the production of different forms of prolamins microstructures with improved functionality for various different applications, including biomaterials and gluten-like networks, for viscoelastic dough.

## MATERIALS AND METHODS

**Materials.** Total kafirin was extracted from decorticated white, tannin non-tannin sorghum grain as described.<sup>32</sup>  $\gamma$ -Kafirin was isolated from total kafirin using 0.05 M sodium lactate containing 2% (v/v) 2-mercaptoethanol<sup>33,34</sup> at a protein/solvent ratio of 1:5. Briefly, total kafirin was mixed with a solution containing 2% (v/v) 2-mercaptoethanol in 0.05 M sodium lactate for 1 h at 25 °C with constant stirring. The mixture was centrifuged at 7200g for 10 min, and the supernatant was collected. The extraction process was repeated twice on the residual pellet, and the supernatants bulked. The supernatant was dialyzed against distilled water for 36 h at 10 °C using dialysis tubing with a 12–14 kDa cut off (Visking ex Labretoria, Pretoria, South Africa) with frequent changes of water. The dialyzed

material ( $\gamma$ -kafirin) and residual pellet (referred to as residual kafirin) were freeze-dried.

**Preparation of Kafirin Microparticles.** Microparticles were prepared by simple coacervation, which is a controlled precipitation of a polymeric solution by adding an incompatible solvent.<sup>35</sup> Microparticles were produced from a solution of kafirin or residual kafirin with 0, 15, and 30% (as a proportion of the total kafirin protein content)  $\gamma$ -kafirin added back, in glacial acetic acid according to Taylor et al.,<sup>3</sup> as modified.<sup>36</sup> This resulted in microparticles suspended in 5.4% acetic acid.

**Sodium Dodecyl Sulfate–Polyacrylamide Gel Electrophoresis (SDS–PAGE).** Kafirin samples and microparticles made from them were characterized using SDS–PAGE under non-reducing and reducing conditions on pre-prepared 4–12% Bis-Tris (BT) gradient gels (Invitrogen Life Technologies, Carlsbad, CA) using an X Cell SureLock Mini-Cell electrophoresis unit (Invitrogen Life Technologies). Kafirin microparticles were washed 3 times with distilled water to remove the acetic acid prior to SDS–PAGE. The protein loading was  $\approx 10 \mu\text{g}$ . Invitrogen Mark12 Unstained Standard was used. Protein bands were stained with Coomassie Brilliant Blue R-250 and photographed using a flat-bed scanner.

**Microscopy. Electron Microscopy.** For high-resolution scanning electron microscopy (SEM) imaging, the microparticle suspensions in distilled water were pipetted on microscope coverslips mounted on an aluminum stub, air-dried, coated with carbon, and viewed with a Zeiss Ultra-Plus 55 FEG-SEM (Oberkochen, Germany) using an accelerating voltage of 1 kV. Transmission electron microscopy (TEM) samples were prepared by pipetting the microparticle suspensions directly onto copper microgrids coated with carbon film and air-dried. Viewing was by a JEM-2100F field emission electron microscope (JEOL, Tokyo, Japan) with an accelerating voltage of 200 kV.

**Atomic Force Microscopy.** Microparticle suspensions in distilled water were pipetted on mica and air-dried. Samples were viewed with a Veeco Icon Dimension atomic force microscope (Bruker, Cambridge,

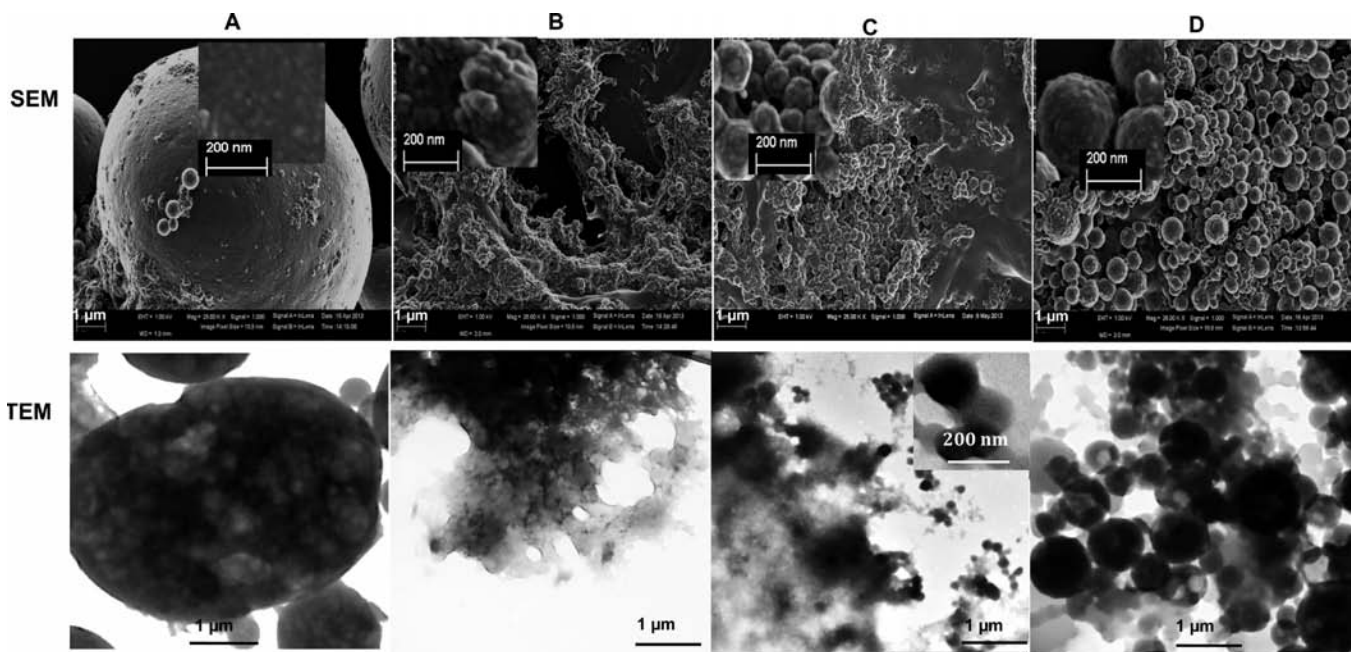


**Figure 2.** Effects of adding  $\gamma$ -kafirin to residual kafirin on the morphology of air-dried kafirin microparticles as examined by electron microscopy: (A) total kafirin microparticles, (B) residual kafirin “microparticles”, (C) residual kafirin + 15%  $\gamma$ -kafirin microparticles, and (D) residual kafirin + 30%  $\gamma$ -kafirin microparticles. The insets are higher magnifications. SEM, scanning electron microscopy; TEM, transmission electron microscopy.

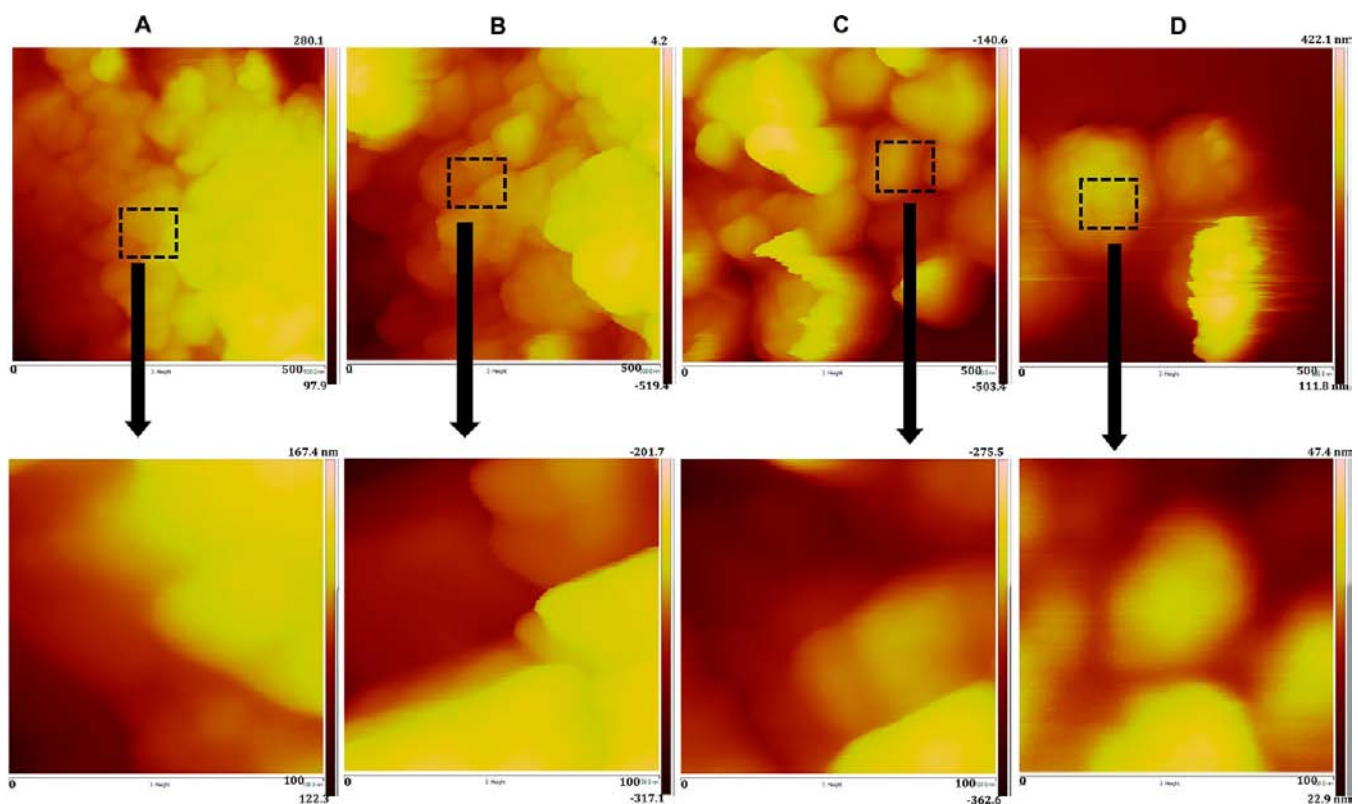


**Figure 3.** Effects of adding  $\gamma$ -kafirin to residual kafirin on the morphology of air-dried kafirin microparticles as examined by AFM: (A) total kafirin microparticles, (B) residual kafirin “microparticles”, (C) residual kafirin + 15%  $\gamma$ -kafirin microparticles, and (D) residual kafirin + 30%  $\gamma$ -kafirin microparticles. Higher magnifications of the regions inside the frame are shown at the bottom.

U.K.) using ScanAsyst (peak force tapping) mode.<sup>37</sup> A 2 nm silicon tip on a nitride lever cantilever was used.

**Fourier Transform Infrared Spectroscopy (FTIR).** Protein secondary structures were determined by FTIR as described.<sup>3</sup> Freeze-dried kafirin microparticles were further dried in a desiccator

containing silica gel for 72 h and then scanned using a Vertex 70v FTIR spectrophotometer (Bruker Optik, Ettlingen, Germany), using 64 scans, 8  $\text{cm}^{-1}$  bandwidth, and an interval of 1  $\text{cm}^{-1}$  in the attenuated total reflectance (ATR) mode in the wavenumber range of 600–4000  $\text{cm}^{-1}$ . The FTIR spectra were normalized and Fourier-



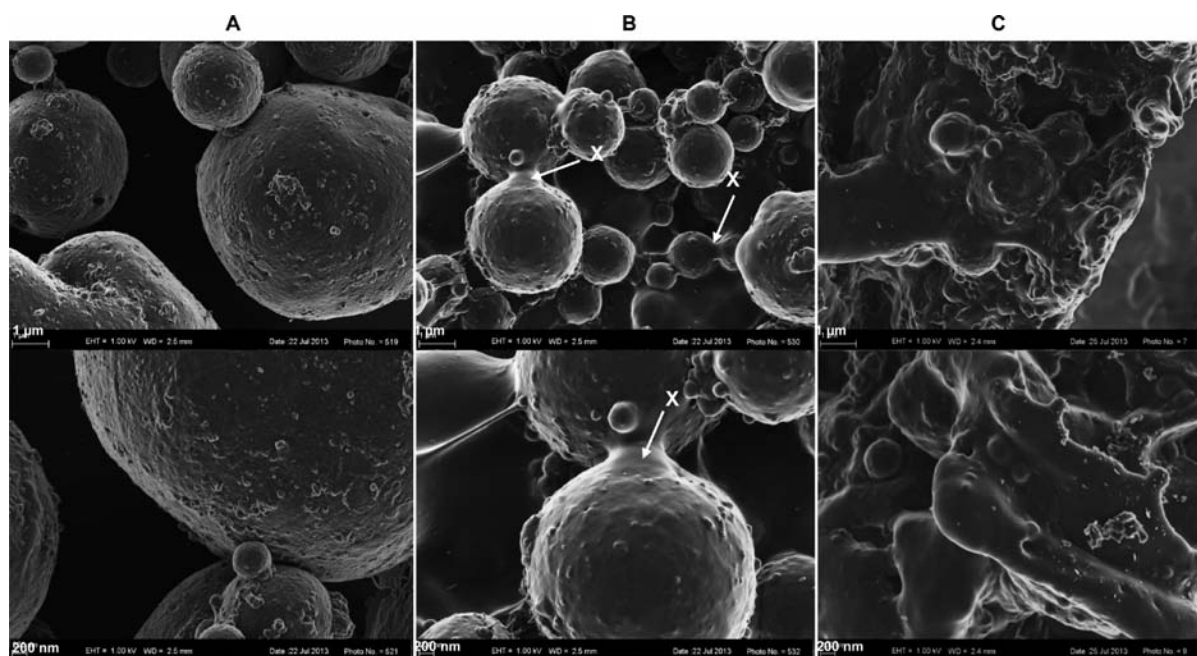


**Figure 4.** Effects of adding  $\gamma$ -kafirin to total kafirin on the morphology of air-dried kafirin microparticles as examined by scanning electron microscopy: (A) total kafirin microparticles, (B) total kafirin + 15%  $\gamma$ -kafirin microparticles (“X” marks the connection point), and (C) total kafirin + 30%  $\gamma$ -kafirin microparticles. The bottom images are higher magnifications.

deconvoluted using Lorentzian filter with a resolution enhancement factor of 2 and 8  $\text{cm}^{-1}$  bandwidth.

**Differential Scanning Calorimetry (DSC).** Thermal analysis was performed by DSC using a Mettler Toledo HP DSC827<sup>e</sup> (Schwerzenbach, Switzerland). Freeze-dried samples were further dried in a desiccator containing silica gel for 14 days. Samples of approximately 15 mg were accurately weighed into 100  $\mu\text{L}$  aluminum pans and sealed immediately. Calibration was based on pure indium. An empty pan was used as a reference. DSC scans were performed from 25 to 280  $^{\circ}\text{C}$  and a heating rate of 10  $^{\circ}\text{C}/\text{min}$  under nitrogen (40 bar pressure). Glass transition ( $T_g$ ) peaks were taken at the peak of step change in heat flow during heating and determined using STAR<sup>e</sup> software, version 9.20.<sup>38,39</sup>

**Statistical Analysis.** Experiments were repeated at least once, except for FTIR and DSC, which were repeated 3 times. Data were analyzed by one-way analysis of variance (ANOVA). Significant differences among the means were determined by Fischer’s least significant difference (LSD) test ( $p < 0.05$ ).

## RESULTS AND DISCUSSION

**SDS–PAGE of Kafirin Proteins.** SDS–PAGE under non-reducing conditions of the isolated  $\gamma$ -kafirin revealed that it had a major  $\gamma$ -kafirin band (approximately 28 kDa) and a fainter band (approximately 46 kDa), equivalent to the minor  $\gamma$ -kafirin band (approximately 49 kDa) described by Evans et al.,<sup>33</sup> both of which have been assigned to the  $\gamma$ -kafirin class.<sup>40</sup> Additionally, there were disulfide cross-linked oligomers of increasing molecular size (lane 3 of gel A in Figure 1). The residual kafirin did not show the 28 kDa  $\gamma$ -kafirin band or 46 kDa band (lane 2 of gels A and B in Figure 1). The total kafirin (lane 1 of gels A and B in Figure 1) differed from the residual kafirin in that it exhibited a more intense monomer band, indicative of the presence of  $\gamma$ -kafirin. Thus, the  $\gamma$ -kafirin extraction was effective.

**Effect of  $\gamma$ -Kafirin on the Morphology of Kafirin “Microparticles”.** When viewed at low magnification, SEM of “microparticles” prepared using residual kafirin appeared as an amorphous mass and lacked discrete shapes (Figure 2B),

indicating failure to organize to the same degree as the total kafirin microparticles (Figure 2A). Higher magnification of residual kafirin “microparticles” showed similar structures to those contained within the larger total kafirin microparticles. Adding 15%  $\gamma$ -kafirin to the residual kafirin resulted in a mixture of non-discrete material and some nanosize discrete spherical structures (Figure 2C). These nanosize particles were not vacuolated, as observed with TEM (see inset picture in Figure 2C). Adding a higher proportion (30%) of  $\gamma$ -kafirin to the residual kafirin resulted in the formation of discrete spherical nanosize particles (Figure 2D). These particles were smaller in size than control total kafirin microparticles, despite the fact that the level of  $\gamma$ -kafirin added was higher than the theoretical 9–12% proportion of  $\gamma$ -kafirin in total kafirin in vitreous (corneous) and 19–21% in opaque sorghum grain endosperm, respectively.<sup>41</sup> The mainly sub-micrometer-sized particles also appeared to be made up of spherical nanostructures, as viewed with high-resolution SEM (see inset pictures in Figure 2). As with the SEM, AFM showed that all kafirin microparticles had a rough surface morphology composed of nanosize protuberances (panels A–D of Figure 3). Similar structures have been reported for kafirin microparticles.<sup>36</sup> AFM of the surface of these nanosize protuberances at higher magnification showed that adding  $\gamma$ -kafirin to residual kafirin, especially at a higher level (30%), resulted in discrete nanoparticles (Figure 3D). This agrees with morphological observation with SEM (Figure 2D).

The addition of 15%  $\gamma$ -kafirin to total kafirin also resulted in relatively smaller microparticles with a smoother surface, which appeared to be connected at the edges (marked with “X”) (Figure 4B). These connections may have been made up of cross-linked  $\gamma$ -kafirin forming a layer on already formed microparticles. There was a loss of the spherical microparticle structure with the addition of 30%  $\gamma$ -kafirin to total kafirin (Figure 4C). This may be due to massive cross-linking and encasing of the kafirin microparticles within the  $\gamma$ -kafirin layer,

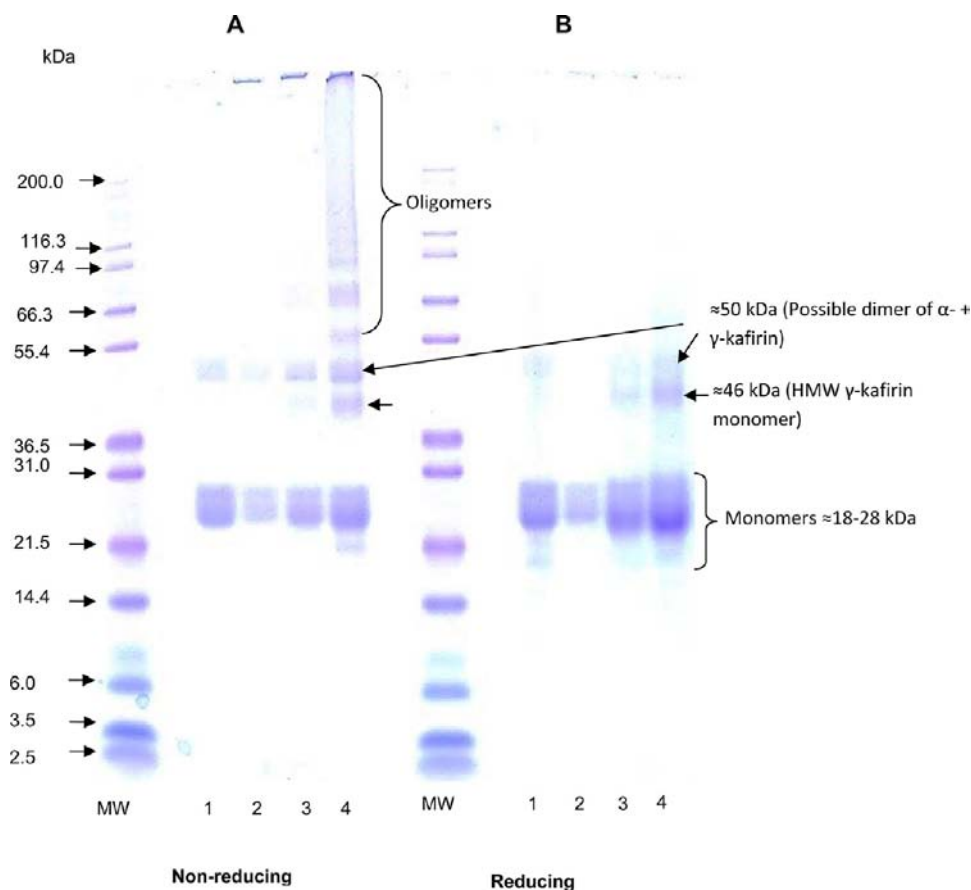


**Figure 5.** SDS-PAGE under (A) non-reducing and (B) reducing conditions of kafirin microparticles. Protein loading  $\approx 10 \mu\text{g}$ . Lanes MW, molecular markers; 1, total kafirin; 2, residual kafirin; 3, residual kafirin + 15%  $\gamma$ -kafirin; and 4, residual kafirin + 30%  $\gamma$ -kafirin.

resulting in the loss of the spherical structures. An attempt to prepare microparticles from isolated  $\gamma$ -kafirin using the simple coacervation technique did not yield microparticles (data not shown). This was probably because isolated  $\gamma$ -kafirin is water-soluble.<sup>33</sup> Hence, the protein could not be precipitated out in the simple coacervation technique applied.

From these microscopy data, it seems that removal of the cysteine-rich  $\gamma$ -kafirin from total kafirin prevents the formation of spherical kafirin microparticles. Possibly,  $\gamma$ -kafirin is needed to stabilize the other  $\alpha$ -,  $\beta$ -, and  $\delta$ -kafirin classes, which may be centrally located within the microparticle. Without this, the structure of the microparticles would be destabilized, as demonstrated. This suggestion is based on a model for kafirin microparticles formation<sup>17</sup> using an analogy of protein body formation but in an isolated and non-cellular system. The model describes that the microparticles form by precipitation of  $\alpha$ - and  $\beta$ -kafirin around small particles of undissolved kafirin and then  $\gamma$ -kafirin forms a stabilizing layer on the surface of the partially formed microparticle. The loss of spherical shape has been observed with both kafirin and zein protein bodies, where downregulating the synthesis of the  $\gamma$ -prolamin class resulted in protein bodies with irregular morphology.<sup>25–29,42</sup> It has been suggested that  $\gamma$ -prolamin plays a role of encasing the other prolamin classes through disulfide cross-linking, thereby preventing the formation of irregular-shaped protein bodies.<sup>42</sup> The fact that the microparticles prepared from residual kafirin with  $\gamma$ -kafirin added were far smaller than total kafirin microparticles suggests that the interaction of the pre-isolated kafirin proteins may not be optimal compared to innate  $\gamma$ -

kafirin in total kafirin. This is probably because the process of isolating the different kafirin classes may have induced changes to these proteins, as was indicated from the SDS-PAGE of  $\gamma$ -kafirin (Figure 1). In terms of kafirin microparticle formation and organization, it seems that  $\gamma$ -kafirin together with  $\beta$ -kafirin could initiate organization of the kafirin microparticles, while the other classes (primarily  $\alpha$ -kafirin) may enlarge the microparticles. The fact that these kafirin microparticles appear to be made up of spherical nanoparticles agrees with the findings by Wang and Padua,<sup>21</sup> who worked on zein microspheres prepared by evaporation-induced self-assembly. According to these authors, a sphere seems to be the basis for all the other microphases produced by self-assembly of zein, the homologue of kafirin.

For the nanosized particles prepared using residual kafirin with 30%  $\gamma$ -kafirin added, the higher resolution AFM of total kafirin microparticles did not show distinct nanostructures. It seems that pre-isolation of  $\gamma$ -kafirin and then adding it to the residual kafirin may have resulted in uneven distribution of  $\gamma$ -kafirin in the resultant microstructure. The residual kafirins could have already interacted with each other prior to commencement of microparticle formation. This was indicated by SEM of microparticles prepared using total kafirin with added  $\gamma$ -kafirin, where  $\gamma$ -kafirin appeared to form a layer on the surface of the microparticles. An uneven distribution of  $\gamma$ -kafirin, which encases the residual kafirin classes would probably result in a clear demarcation. The demarcations would be created by the  $\gamma$ -kafirin layer occurring on the surface of each of the nanostructures that constitute the microparticle.

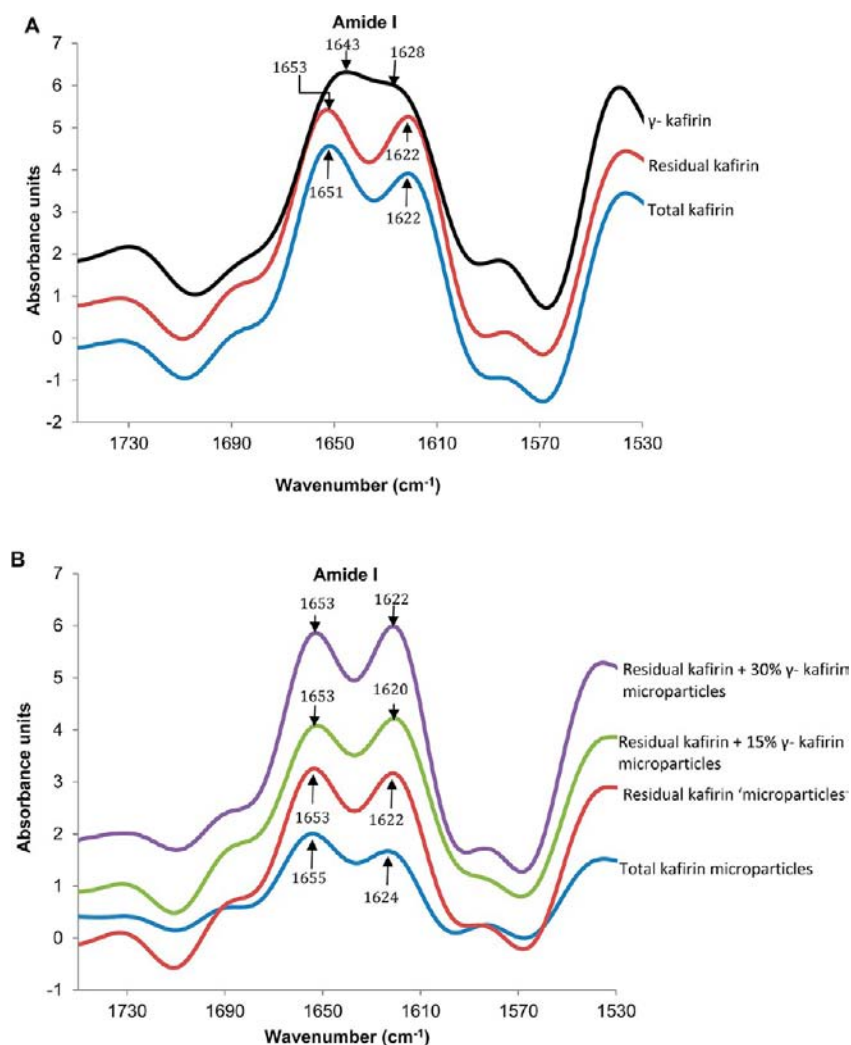


**Figure 6.** FTIR spectra of kafirin and air-dried kafirin microparticles: (A) total kafirin, residual kafirin, and  $\gamma$ -kafirin proteins and (B) kafirin microparticles. Spectra were offset for clarity.

Alternatively, during formation of microparticles with total kafirin, all of the kafirin classes could interact at virtually the same time. Hence, the distribution of  $\gamma$ -kafirin in the total kafirin microparticle would be more even, resulting in less distinct boundaries between the nanosized structures.

An unresolved finding from this study is that, while commercial zein, which is essentially only  $\alpha$ -zein,<sup>43</sup> can form distinct spherical microparticles<sup>44</sup> in the absence of the  $\gamma$ -prolamin class, kafirin did not form discrete microparticles. This suggests that other factors besides the absence of the  $\gamma$ -prolamin class are involved. First, it is known that commercial zeins are variable<sup>45</sup> and, hence, may contain small amounts of the other zein classes. Second, it has been proposed that  $\alpha$ -zein has lutein at the core of its triple helical segments,<sup>46</sup> which helps to stabilize the protein configuration<sup>46</sup> and, thereby, could stabilize  $\alpha$ -zein microparticles.

**Effects of  $\gamma$ -Kafirin on the Chemical Structure of Kafirin "Microparticles".** SDS-PAGE under non-reducing conditions of the kafirin "microparticles" showed that there was an increase in oligomer bands as a result of the addition of  $\gamma$ -kafirin to the residual kafirin (gel A in Figure 5). A band  $\approx 50$  kDa, which is likely to be a dimer of  $\alpha$ -kafirin ( $\approx 22$  kDa) and  $\gamma$ -kafirin ( $\approx 28$  kDa),<sup>40</sup> was noted for microparticles prepared using residual kafirin with added  $\gamma$ -kafirin (lanes 3 and 4 of gel

A in Figure 5). However, the oligomer bands were faint under reducing conditions, indicating that the polymerization as a result of the addition of  $\gamma$ -kafirin was due to disulfide cross-linking and that the linkages were broken by the reducing agent, as demonstrated by the increase in intensity of kafirin monomeric bands (lanes 3 and 4 of gel B in Figure 5). There were no dimer and oligomer bands in the absence of  $\gamma$ -kafirin with SDS-PAGE of residual kafirin microparticles under reducing conditions (lane 2 of gel B of Figure 5). This shows the importance of  $\gamma$ -kafirin in polymerization of kafirin proteins. In contrast, kafirin dimers resistant to reduction by mercaptoethanol were observed with microparticles prepared using either total kafirin or residual kafirin with  $\gamma$ -kafirin added (lanes 1, 3, and 4 of gel B in Figure 5). Similar reduction resistant bands were observed with kafirin microparticle films.<sup>47</sup> It has been suggested that the presence of polymeric kafirin resistant to reduction could be due to some covalent cross-links being inaccessible to the reducing agent.<sup>19</sup>

Isolated  $\gamma$ -kafirin showed two peaks in the amide I region as determined by FTIR with normalization and resolution enhancement using Fourier deconvolution (Figure 6A). The higher peak at  $1643\text{ cm}^{-1}$  was assigned to random-coil conformation, and the lower peak at  $1628\text{ cm}^{-1}$  was assigned to antiparallel  $\beta$ -sheet conformation.<sup>48–50</sup> It is possible that the

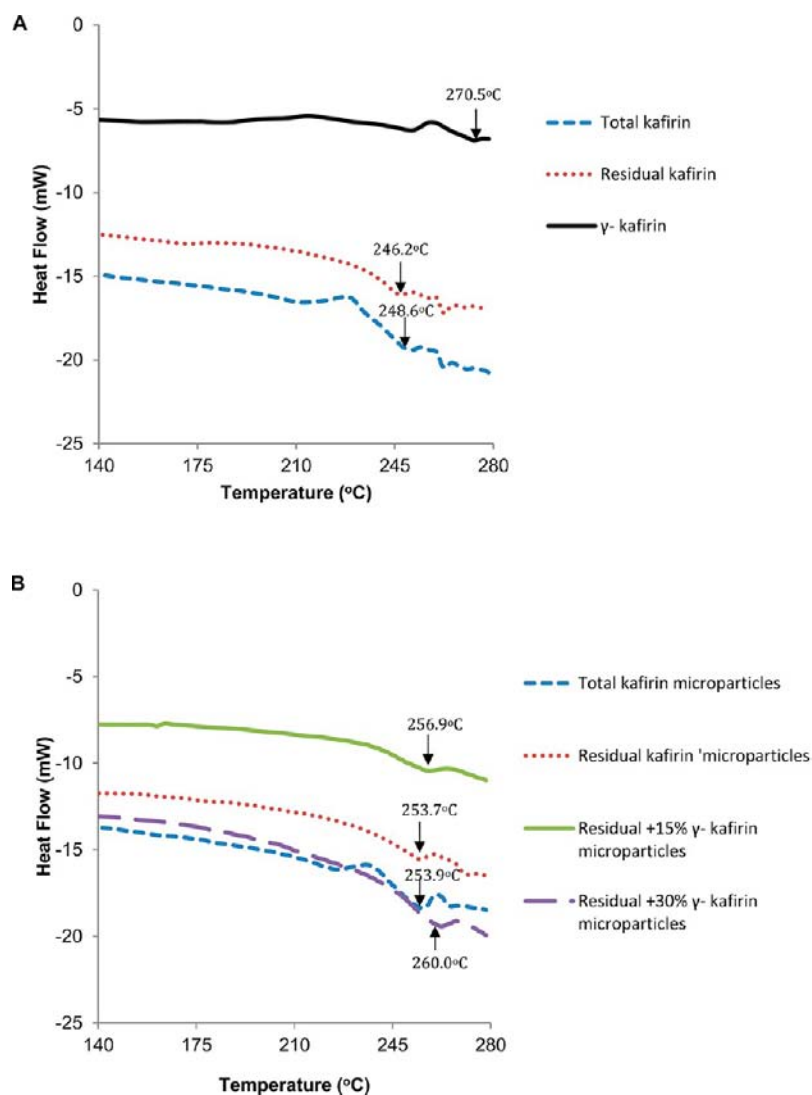


**Figure 7.** Typical DSC thermograms of kafirin proteins and kafirin microparticles: (A) proteins and (B) microparticles. Arrows mark melting temperatures, which are probably  $T_g$ .

$\beta$ -sheet component could contain some polyproline II (PPII) conformation, because PPII cannot be measured by solid-state FTIR because the  $\beta$ -sheet and PPII signals overlap.<sup>51</sup>  $\gamma$ -Kafirin and  $\gamma$ -zein both have repeats of a conserved hexapeptide motif (PPPVHL) in the N-terminal domain,<sup>18</sup> and therefore,  $\gamma$ -kafirin may be expected to exhibit some PPII conformation, as reported for  $\gamma$ -zein.<sup>51</sup> However, Bansal et al.<sup>52</sup> using a PSIPRED protein structure prediction server for  $\gamma$ -kafirin also reported a large proportion of coil (82.79%), with a small amount of helix (11.83%) and extended strand (5.38%) but no  $\beta$ -sheet. In contrast, the secondary structure of  $\gamma$ -zein has been shown to contain 33% helix and 31%  $\beta$ -sheet when analyzed in the solid state by FTIR.<sup>53</sup>

FTIR spectra of kafirin microparticles and residual kafirin “microparticles” both showed two peaks at wavenumbers between 1653 and 1655 and between 1622 and 1624 in the amide I region (Figure 6B), which can be assigned to  $\alpha$ -helical conformation and antiparallel  $\beta$ -sheet conformation, respectively.<sup>48</sup> However, the ratio of  $\alpha$ -helical to  $\beta$ -sheet differed. For the total kafirin microparticles, this ratio was 1.2, which was similar to the 1.3 reported by Taylor et al.<sup>3</sup> for kafirin microparticles. The ratio of  $\alpha$ -helical to  $\beta$ -sheet for residual

kafirin “microparticles”, 1.06, indicated a greater proportion of  $\beta$ -sheet. Adding  $\gamma$ -kafirin to the residual kafirin and using the resultant kafirin mixture to prepare microparticles indicated a further small decrease in the ratio of  $\alpha$ -helical to  $\beta$ -sheet to 0.99 and 0.98 when 15 and 30%  $\gamma$ -kafirin were added back, respectively. An increase in the relative proportion of  $\beta$ -sheet structures has been associated with disulfide cross-linking of kafirin proteins.<sup>48</sup>

**Effect of  $\gamma$ -Kafirin on the Thermal Properties of Kafirin “Microparticles”.** DSC showed that  $\gamma$ -kafirin had significantly higher  $T_g$  ( $p < 0.05$ ) compared to total kafirin and residual kafirin (Figure 7A). This may be due to the high cysteine residue content of  $\gamma$ -kafirin, about 7 mol %, <sup>18</sup> resulting in a greater extent of disulfide cross-linking. To the best of the authors’ knowledge, this is also the first report of  $T_g$  of  $\gamma$ -kafirin. Adding  $\gamma$ -kafirin to residual kafirin increased the kafirin microparticle  $T_g$  significantly ( $p < 0.05$ ) (Figure 7B). The increase in  $T_g$  was likely also due to the increase in disulfide cross-linking.<sup>54</sup> The microparticles had significantly higher  $T_g$  ( $p < 0.05$ ) (Figure 7B) compared to proteins from which they were prepared (Figure 7A), probably because of the increase in the relative proportion of the  $\beta$ -sheet conformation during



microparticle formation. Because  $\beta$ -sheet conformations are associated with protein unfolding,<sup>48</sup> alignment of these protein molecules may result in an increase in disulfide cross-linking or hydrogen bonding, thereby increasing  $T_g$ . The  $T_g$  value for total kafirin in the present study ( $\approx 248$  °C) was higher than the  $\approx 230$  °C reported by Wang et al.,<sup>55</sup> possibly because of differences in moisture contents. In the present study, the freeze-dried samples were dried further in a desiccator for over 2 weeks, while in the Wang et al.<sup>55</sup> study, the samples were not further dried. The moisture content is known to strongly affect  $T_g$  of prolamin proteins<sup>56–58</sup> by acting as a plasticizer.

This work has demonstrated that the  $\gamma$ -kafirin class is required to form spherical kafirin microstructures (microparticles). It stabilizes their structure because of its ability to form disulfide cross-links, probably encasing the other kafirin classes in a similar manner to that which occurs in prolamin protein bodies.<sup>42</sup> Adding  $\gamma$ -kafirin to total kafirin does not result in larger particles because the excess cross-linking by  $\gamma$ -kafirin seems to create an imbalance among the forces that maintain the spherical microparticle shape, thereby destabilizing the microparticle structure. The work has presented for the first time  $T_g$  data of isolated  $\gamma$ -kafirin, which shows that its  $T_g$  is higher than that of total kafirin and residual kafirin. This improved understanding on the role of the  $\gamma$ -prolamin class in kafirin microstructures and knowledge on the secondary structure and thermal properties of isolated  $\gamma$ -kafirin will be useful in the development of kafirin or zein bioplastics with functional properties that are more comparable to synthetic polymer plastics.

## AUTHOR INFORMATION

### Corresponding Author

\*Telephone: +27-12-420-5402. Fax: +27-12-420-2839. E-mail: janet.taylor@up.ac.za.

### Funding

Joseph Anyango is grateful for the provision of a University of Pretoria Postdoctoral Fellowship.

### Notes

The authors declare no competing financial interest.

## ACKNOWLEDGMENTS

We thank A. Hall, C. van der Merwe, A. Botha, and A. Buys for their assistance with microscopy.

## ABBREVIATIONS USED

SDS–PAGE, sodium dodecyl sulfate–polyacrylamide gel electrophoresis; SEM, scanning electron microscopy; TEM, transmission electron microscopy; AFM, atomic force microscopy; DSC, differential scanning calorimetry; FTIR, Fourier transform infrared spectroscopy;  $T_g$ , glass transition temperature

## REFERENCES

- (1) Parris, N.; Cooke, P. H.; Hicks, K. B. Encapsulation of essential oils in zein nanospherical particles. *J. Agric. Food Chem.* **2005**, *53*, 4788–4792.
- (2) Wang, H. J.; Lin, Z. X.; Liu, X. M.; Sheng, S. H.; Wang, J. Y. Heparin-loaded zein microsphere film and hemocompatibility. *J. Controlled Release* **2005**, *105*, 120–131.
- (3) Taylor, J.; Taylor, J. R. N.; Belton, P. S.; Minnaar, A. Formation of kafirin microparticles by phase separation from an organic acid and their characterisation. *J. Cereal Sci.* **2009**, *50*, 99–105.

- (4) Gao, C.; Taylor, J.; Wellner, N.; Byaruhanga, Y. B.; Parker, M. L.; Mills, E. N. C.; Belton, P. S. Effect of protein secondary structure and biofilm formation of kafirin. *J. Agric. Food Chem.* **2005**, *52*, 2382–2385.
- (5) Torres-Giner, S.; Gimenez, E.; Lagaron, J. M. Characterization of the morphology and thermal properties of zein prolamin nanostructures obtained by electrospinning. *Food Hydrocolloids* **2008**, *22*, 601–614.
- (6) Wang, Y.; Chen, L. Electrospinning of prolamin proteins in acetic acid: The effects of protein conformation and aggregation in solution. *Macromol. Mater. Eng.* **2012**, *297*, 902–913.
- (7) Padua, G. W.; Wang, Q.; Wang, Y. Construction and properties of zein-based cell supports and scaffolds. *Nanotech. Conf. Expo 2010* **2010**, *3*, 202–205.
- (8) Gong, S.; Wang, H.; Sun, Q.; Xue, S.-T.; Wang, J.-Y. Mechanical properties and in vitro biocompatibility of porous zein scaffolds. *Biomaterials* **2006**, *27*, 3793–3799.
- (9) Erickson, D. P.; Campanella, O. H.; Hamaker, B. R. Functionalizing maize zein in viscoelastic dough systems through fibrous,  $\beta$ -sheet-rich protein networks: An alternative, physicochemical approach to gluten-free breadmaking. *Trends Food Sci. Technol.* **2012**, *24*, 74–81.
- (10) Tu, J.; Wang, H.; Li, H.; Wang, J.; Zhang, X. The *in vivo* bone formation by mesenchymal stem cells in zein scaffolds. *Biomaterials* **2009**, *30*, 4369–4376.
- (11) Liu, X.; Sun, Q.; Wang, H.; Zhang, J. Y. Microspheres of corn protein, zein, for ivermectin drug delivery system. *J. Controlled Release* **2005**, *26*, 102–131.
- (12) Taylor, J.; Taylor, J. R. N.; Belton, P. S.; Minnaar, A. Kafirin microparticle encapsulation of catechin and sorghum condensed tannins. *J. Agric. Food Chem.* **2009**, *57*, 7523–7528.
- (13) Luo, Y.; Teng, Z.; Wang, Q. Development of zein nanoparticles coated with carboxymethyl chitosan for encapsulation and controlled release of vitamin D3. *J. Agric. Food Chem.* **2012**, *60*, 836–843.
- (14) Mejia, C. D.; Mauer, L. J.; Hamaker, B. R. Similarities and differences in secondary structure of viscoelastic polymers of maize  $\alpha$ -zein and wheat gluten proteins. *J. Cereal Sci.* **2007**, *45*, 353–359.
- (15) Mejia, C. D.; Gonzalez, D. C.; Mauer, L. J.; Campanella, O. H.; Hamaker, B. R. Increasing and stabilizing  $\beta$ -sheet structure of maize zein causes improvement in its rheological properties. *J. Agric. Food Chem.* **2012**, *60*, 2316–2321.
- (16) Buchner, S.; Kinnear, M.; Crouch, I. J.; Taylor, J.; Minnaar, A. Extending the post-harvest sensory quality and shelf-life of 'Packham's Triumph' pears with a kafirin protein coating. *J. Sci. Food Agric.* **2011**, *91*, 2814–2820.
- (17) Taylor, J.; Anyango, J. O.; Taylor, J. R. N. Developments in the science of zein, kafirin and gluten protein bio-plastic materials. *Cereal Chem.* **2013**, *90*, 344–357.
- (18) Belton, P. S.; Delgalligo, I.; Halford, N. G.; Shewry, P. R. Kafirin structure and functionality. *J. Cereal Sci.* **2006**, *44*, 272–286.
- (19) Duodu, K. G.; Taylor, J. R. N.; Belton, P. S.; Hamaker, B. R. Factors affecting sorghum protein digestibility. *J. Cereal Sci.* **2003**, *38*, 117–131.
- (20) Wang, Y.; Padua, G. W. Formation of zein microphases in ethanol–water. *Langmuir* **2010**, *26*, 12897–12901.
- (21) Wang, Y.; Padua, G. W. Nanoscale characterization of zein self-assembly. *Langmuir* **2012**, *28*, 2429–2435.
- (22) Taylor, J. Preparation, characterisation and functionality of kafirin microparticles. Ph.D. Thesis, University of Pretoria, Pretoria, South Africa, 2008.
- (23) Anyango, J. O. Physico-chemical modification of kafirin microstructures for application as biomaterials. Ph.D. Thesis, University of Pretoria, Pretoria, South Africa, 2012.
- (24) Shull, J. M.; Watterson, J. J.; Kirleis, A. W. Purification and immunocytochemical localisation of kafirins in *Sorghum bicolor* (L. Moench) endosperm. *Protoplasma* **1992**, *171*, 64–74.
- (25) Coleman, C. E.; Herman, E. M.; Takasaki, K.; Larkins, B. A. The maize  $\gamma$ -zein sequesters  $\alpha$ -zein and stabilizes its accumulation in protein bodies of transgenic tobacco endosperm. *Plant Cell* **1996**, *8*, 2335–2345.



- (26) Wu, Y.; Holding, D. R.; Messing, J.  $\gamma$ -Zeins are essential for endosperm modification in quality protein maize. *Proc. Natl. Acad. Sci. U. S. A.* **2010**, *107*, 12810–12815.
- (27) Da Silva, L. S.; Jung, R.; Zhao, Z.; Glassman, K.; Taylor, J.; Taylor, J. R. N. Effect of suppressing the synthesis of different kafirin sub-classes on grain endosperm texture, protein body structure and protein nutritional quality in improved sorghum lines. *J. Cereal Sci.* **2011**, *54*, 160–167.
- (28) Da Silva, L. S.; Taylor, J.; Taylor, J. R. N. Transgenic sorghum with altered kafirin synthesis: Kafirin solubility, polymerization and protein digestion. *J. Agric. Food Chem.* **2011**, *59*, 9265–9270.
- (29) Kumar, T.; Dweikat, I.; Sato, S.; Ge, Z.; Nersesian, N.; Chen, H.; Elthon, T.; Bean, S.; Ioerger, B. P.; Tilley, M.; Clemente, T. Modulation of kernel storage proteins in grain sorghum (*Sorghum bicolor* (L.) Moench. *Plant Biotech. J.* **2012**, *10*, 533–544.
- (30) Schober, T. J.; Bean, S. R.; Tilley, M.; Smith, B. M.; Ioerger, B. P. Impact of different isolation procedures on the functionality of zein and kafirin. *J. Cereal Sci.* **2011**, *54*, 241–249.
- (31) Reis, C. P.; Neufeld, R. J.; Ribeiro, A. J.; Veiga, F. Nanoencapsulation II. Biomedical applications and current status of peptide and protein nanoparticulate delivery systems. *Nanomed. Nanotechnol. Biol. Med.* **2006**, *2*, 53–65.
- (32) Emmambux, N. M.; Taylor, J. R. N. Sorghum kafirin interaction with various phenolic compounds. *J. Sci. Food Agric.* **2003**, *83*, 402–407.
- (33) Evans, D. J.; Schüssler, L.; Taylor, J. R. N. Isolation of reduced-soluble protein from sorghum starchy endosperm. *J. Cereal Sci.* **1987**, *5*, 61–67.
- (34) Taylor, J.; Bean, S. R.; Ioerger, B. P.; Taylor, J. R. N. Preferential binding of sorghum tannins with  $\gamma$ -kafirin and the influence of tannin binding on kafirin digestibility and biodegradation. *J. Cereal Sci.* **2007**, *46*, 22–31.
- (35) Mathiowitz, E.; Kreitz, M. R.; Brannon-Peppas, L. Microencapsulation. In *Encyclopedia of Controlled Drug Delivery*; Mathiowitz, E., Ed.; John Wiley and Sons, Inc.: New York, 1999; Vol. 1, pp 493–546.
- (36) Anyango, J. O.; Duneas, N.; Taylor, J. R. N.; Taylor, J. Physicochemical modification of kafirin microparticles and their ability to bind bone morphogenetic protein-2 (BMP-2), for application as a biomaterial. *J. Agric. Food Chem.* **2012**, *60*, 8419–8426.
- (37) Kaemmer, S. B. *Introduction to Bruker's ScanAsyst and PeakForce Tapping AFM Technology*; Bruker Nano, Inc.: Santa Barbara, CA, 2011; Bruker Application Note 133.
- (38) Thermal Analysis UserCom 11. *Interpreting DSC Curves. Part 1: Dynamic Measurements. Information for Users of Mettler Toledo Thermal Analysis System*, 1/2000 ([http://uk.mt.com/dam/non-indexed/po/ana/ta-usercom/51710020\\_UserCom11\\_TA\\_e.pdf](http://uk.mt.com/dam/non-indexed/po/ana/ta-usercom/51710020_UserCom11_TA_e.pdf)) (accessed Aug 2013).
- (39) Wang, Y.; Rakotonirainy, A. M.; Padua, G. W. Thermal behavior of zein-based biodegradable films. *Starch/Staerke* **2003**, *55*, 25–29.
- (40) El Nour, N. A.; Peruffo, A. D. B.; Curioni, A. Characterisation of sorghum kafirins in relations to their cross-linking behavior. *J. Cereal Sci.* **1998**, *28*, 197–207.
- (41) Oria, M. P.; Hamaker, B. R.; Axtell, J. D.; Huang, C.-P. A highly digestible sorghum mutant cultivar exhibits a unique folded structure of endosperm protein bodies. *Proc. Natl. Acad. Sci. U. S. A.* **2000**, *97*, 5065–5070.
- (42) Wu, Y.; Messing, J. RNA interference-mediated change in protein body morphology and seed opacity through loss of different zein proteins. *Plant Physiol.* **2010**, *153*, 337–347.
- (43) Lawton, J. W. Zein: A history of processing and use. *Cereal Chem.* **2002**, *79*, 1–18.
- (44) Zhong, Q.; Jin, M. Zein nanoparticles produced by liquid–liquid dispersion. *Food Hydrocolloids* **2009**, *23*, 2380–2387.
- (45) Selling, G. W.; Lawton, J.; Bean, S.; Dunlap, C.; Sessa, D. J.; Willett, J. L.; Byars, J. Rheological studies utilizing various lots of zein in *N,N*-dimethylformamide solutions. *J. Agric. Food Chem.* **2005**, *53*, 9050–9055.
- (46) Momany, F. A.; Sessa, D. J.; Lawton, J. W.; Selling, G. W.; Hamaker, S. A. H.; Willet, J. L. Structural characterization of  $\alpha$ -zein. *J. Agric. Food Chem.* **2006**, *54*, 543–547.
- (47) Anyango, J. O.; Taylor, J.; Taylor, J. R. N. Improvement in water stability and other related functional properties of thin cast kafirin films. *J. Agric. Food Chem.* **2011**, *59*, 12674–12682.
- (48) Duodu, K. G.; Tang, H.; Grant, A.; Wellner, N.; Belton, P. S.; Taylor, J. R. N. FTIR and solid state  $^{13}\text{C}$  NMR spectroscopy of proteins of wet cooked and popped sorghum and maize. *J. Cereal Sci.* **2001**, *33*, 261–269.
- (49) Mizutani, Y.; Matsumura, Y.; Imamura, K.; Nakanishi, K.; Mori, T. Effects of water activity and lipid addition on secondary structure of zein in powder systems. *J. Agric. Food Chem.* **2003**, *51*, 229–235.
- (50) Kong, J.; Yu, S. Fourier transform infrared spectroscopic analysis of protein secondary structures. *Acta Biochim. Biophys. Sin.* **2007**, *39*, 579–559.
- (51) Bicudo, T. C.; Bicudo, R. C.; Forato, L. A.; Beltrami, L. M.; Batista, L. A.; Filho, R. B.; Colnago, L. A.  $\gamma$ -Zein secondary structure in solution by circular dichroism. *Biopolymers* **2008**, *89*, 175–178.
- (52) Bansal, S.; Mishra, A.; Tomar, A.; Sharma, S.; Khanna, V. K.; Garg, G. K. Isolation and temporal endospermal expression of  $\gamma$ -kafirin gene of grain sorghum (*Sorghum bicolor* L. moench) var. M 35-1 for introgression analysis of transgene. *J. Cereal Sci.* **2008**, *48*, 808–815.
- (53) Bicudo, T. C.; Forato, L. A.; Batista, L. A. R.; Colnago, L. A. Study of the conformation of  $\gamma$ -zeins in purified maize protein bodies by FTIR and NMR spectroscopy. *Anal. Bioanal. Chem.* **2005**, *383*, 291–296.
- (54) Matveev, Y. I.; Grinberg, V. Y.; Sochava, I. V.; Tolstoguzov, V. B. Glass transition temperature of proteins. Calculation based on the additive contribution method and experimental data. *Food Hydrocolloids* **1997**, *11*, 125–133.
- (55) Wang, Y.; Tilley, M.; Bean, S.; Sun, X. S.; Wang, D. Comparison of methods for extracting kafirin proteins from sorghum distillers dried grains with solubles. *J. Agric. Food Chem.* **2009**, *57*, 8366–8372.
- (56) Lawton, J. W. Viscoelasticity of zein-starch doughs. *Cereal Chem.* **1992**, *69*, 351–355.
- (57) De Graaf, E. M.; Madeka, H.; Cocero, A. M.; Kokini, J. L. Determination of the effect of moisture on gliadin glass transition using mechanical spectrometry and differential scanning calorimetry. *Biotechnol. Prog.* **1993**, *9*, 210–213.
- (58) Madeka, H.; Kokini, J. L. Effect of glass transition and cross-linking on rheological properties of zein: Development of a preliminary state diagram. *Cereal Chem.* **1996**, *73*, 433–438.